Applied Microbiology and Biotechnology (2020) 104:6429–6441
https://doi.org/10.1007/s00253-020-10735-4

MINI-REVIEW

Ribose-5-phosphate isomerases: characteristics, structural features, and applications

Jiajun Chen[1] · Hao Wu[1] · Wenli Zhang[1,2] · Wanmeng Mu[1,2]

Received: 1 April 2020 / Revised: 2 June 2020 / Accepted: 7 June 2020 / Published online: 12 June 2020

Abstract

Ribose-5-phosphate isomerase (Rpi, EC 5.3.1.6) is widespread in microorganisms, animals, and plants. It has a pivotal role in the pentose phosphate pathway and responsible for catalyzing the isomerization between D-ribulose 5-phosphate and D-ribose 5-phosphate. In recent years, Rpi has received considerable attention as a multipurpose biocatalyst for production of rare sugars, including D-allose, L-rhamnulose, L-lyxose, and L-tagatose. Besides, it has been thought of as a potential drug target in the treatment of trypanosomatid-caused diseases such as Chagas' disease, leishmaniasis, and human African trypanosomiasis. Despite increased research activities, up to now, no systematic review of Rpi has been published. To fill this gap, this paper provides detailed information about the enzymatic properties of various Rpis. Furthermore, structural features, catalytic mechanism, and molecular modifications of Rpis are summarized based on extensive crystal structure research. Additionally, the applications of Rpi in rare sugar production and the role of Rpi in trypanocidal drug design are reviewed.

Key points

- *Fundamental properties of various ribose-5-phosphate isomerases (Rpis).*
- *Differences in crystal structure and catalytic mechanism between RpiA and RpiB.*
- *Application of Rpi as a rare sugar producer and a potential drug target.*

Keywords Ribose-5-phosphate isomerase · Substrate specificity · Structural features · Rare sugar · Potential drug target

Introduction

Ribose-5-phosphate isomerase (Rpi, EC 5.3.1.6), the first enzyme of the non-oxidative branch of the pentose phosphate pathway, could reversibly catalyze the interconversion between D-ribulose 5-phosphate (Ru5P) and D-ribose 5-phosphate (R5P) (Stincone et al. 2015) (Fig. S1). It also plays a vital role in the metabolism of D-allose (Poulsen et al. 1999), and the Calvin cycle of photosynthesis (Jung et al. 2000). Rpi exists in two distinct forms, type A (RpiA) and type B (RpiB); although they have the same catalytic function, they are evolutionarily and structurally unrelated to each other. RpiA appears to be ubiquitous in all three kingdoms of life, while RpiB only exists in some bacteria and protozoans (Lobley et al. 2012). Currently, the parasitic trypanosomatid-caused diseases such as Chagas' disease, leishmaniasis, and human African trypanosomiasis have severely threatened human health and economy throughout the world. However, due to the absence of human effective vaccines, current available therapeutic means are restricted to chemotherapy with limited efficacy, resulting in high levels of morbidity and mortality (Kovarova and Barrett 2016). Recently, Rpi has been brought into focus as a potential drug target in the treatment of trypanosomatid-caused diseases. The Rpis of trypanosomatids, which are essential for trypanosomatids survival and/or infectivity, belong to type B, while the Rpis which exist in mammalian hosts are the completely unrelated type A (Sinatti et al. 2017). Therefore, specifically competitive inhibitors of trypanosomatids RpiB appear as promising drugs against trypanosomatids.

In the last two decades, rare sugars, defined by the International Society of Rare Sugar as naturally existing

Electronic supplementary material The online version of this article (https://doi.org/10.1007/s00253-020-10735-4) contains supplementary material, which is available to authorized users.

✉ Wenli Zhang
wenlizhang@jiangnan.edu.cn

[1] State Key Laboratory of Food Science and Technology, Jiangnan University, Wuxi 214122, Jiangsu, China

[2] International Joint Laboratory on Food Safety, Jiangnan University, Wuxi 214122, Jiangsu, China

monosaccharides and their derivatives within very small amount (Izumori 2002), have been studied widely due to the attractive physicochemical properties and physiological functions. D-Allulose and D-tagatose, two most intensively studied rare sugars, have received GRAS (Generally Recognized as Safe) approval from the United States Food and Drug Administration and authorized serving as promising low-calorie sweeteners in the food industry (Zhang et al. 2017). Increasing the availability of rare sugars is an important guarantee for further discovering their new characteristics and applications. Considering that direct extraction is cost-prohibitive, the eco-friendly and highly specific enzymatic approaches are preferred for the mass production of rare sugars (Granstrom et al. 2004). In this context, Rpi, which cannot only catalyze the isomerization reaction between phosphorylated aldoses and ketoses but also isomerize a variety of monosaccharides with the same backbone conformation as the phosphorylated substrates, offers a potential for rare sugar bioproduction. Because of its broad substrate specificity, Rpi has been used for the biotechnological production of D-allose and some other L-form rare monosaccharides like L-rhamnulose, L-lyxose, and L-tagatose. D-Allose, a C3 epimer of D-glucose, is a low-calorie sweetener with various beneficial physiological functions such as antitumor, anticancer, cryoprotection, anti-inflammatory, antihypertension, neuroprotection, antioxidant, antiosteoporosis, and immunosuppression (Chen et al. 2018b). L-Sugars are generally used as essential precursors in the preparation of many valuable compounds. L-Rhamnulose, L-lyxose, and L-tagatose are indispensable starting materials for the synthesis of 2,5-dimethyl-4-hydroxy-3(2H)-furanone (a caramel-like food flavor substance) (Hecquet et al. 1996), avilamycin A (an oligosaccharide antibiotic) (Hofmann et al. 2005), and deoxygalactonojirimycin (a glycosidase inhibitor) (Jenkinson et al. 2011), respectively.

In this review, the first part will present the biochemical characteristics of reported microbial Rpis and compare them in detail. The second part will mainly focus on the structural features, catalytic mechanism, and molecular modifications of Rpis. Finally, recent advances in using Rpi as a powerful biocatalyst for rare sugar bioproduction and as a potential drug target for treatment of trypanosomatid-caused diseases are provided.

Biochemical characteristics of Rpis

Novel enzyme sources

Rpis are widely distributed and generally at least one of the two completely unrelated isoforms, RpiA and RpiB, is present in an organism. So far, microbial RpiA has been identified from *Escherichia coli* K12 (Rangarajan et al. 2002; Zhang et al. 2003a), *Pyrococcus horikoshii* OT3 (Ishikawa et al. 2002), *Thermus thermophilus* HB8 (Hamada et al. 2003), *Saccharomyces cerevisiae* S288C (Graille et al. 2005), *Plasmodium falciparum* 3D7 (Holmes et al. 2006), *Vibrio vulnificus* YJ016 (Kim et al. 2009), *Methanocaldococcus jannaschii* MJ1603 (Strange et al. 2009), and *Lactobacillus salivarius* UCC118 (Lobley et al. 2012). However, these studies have mainly focused on the crystal structure analysis which will be discussed in the next section. Recently, the broad substrate specificity of RpiB towards diverse monosaccharides, which represents a potential for rare sugar production, has attracted ever-increasing attention from researchers. In 2007, Park et al. (2007a) characterized RpiB from *Clostridium thermocellum* ATCC 27405 and experimentally investigated the isomerization capacity of RpiB towards non-phosphorylated substrates for the first time. Subsequently, RpiBs from *Clostridium difficile* ATCC BAA-1382D-5 (Yeom et al. 2010), *Thermotoga maritima* ATCC 43589D-5 (Yeom et al. 2010), *Streptococcus pneumoniae* ATCC BAA-255 (Park et al. 2011), *Thermotoga lettingae* TMO (Feng et al. 2013), and *Ochrobactrum* sp. CSL1 (Shen et al. 2018) were identified one after another. The enzymatic properties of these mentioned RpiBs are summarized in Table 1 and discussed below.

Effect of pH, temperature, and metal ions

To achieve high yields of rare sugar production by RpiB, slightly acidic pH and adequately high temperature are considered as the most favorable conditions for the isomerization, because non-enzymatic browning like Maillard reaction is pH-dependent and will be restrained in a weakly acidic reaction system (Fan et al. 2015; Kwon and Baek 2014). Besides, the relatively elevated reaction temperature can provide several prominent advantages such as high solubility of substrate and product, low viscosity of reaction mixtures, small risk of microbial contamination, and profitable shift of reaction equilibrium (Xu et al. 2016). However, all of the characterized RpiBs exhibited maximal activity under weakly alkaline conditions of pH 7.5–8.0 (Table 1). *T. lettingae* TMO RpiB could maintain 80% of its maximal activity at pH 6.0–9.0 (Feng et al. 2013), while RpiBs from *Ochrobactrum* sp. CSL1 and *S. pneumoniae* ATCC BAA-255 were unstable below pH 7.0 (Park et al. 2011; Shen et al. 2018). Therefore, screening new RpiBs with a slightly acidic optimum pH and/or engineering the pH optimum of characterized RpiBs to lower values are considered necessary in future research.

As shown in Table 1, the optimal temperature for aldose-ketose isomerization catalyzed by different RpiBs varied from 35 to 75 °C. *T. lettingae* TMO RpiB and *S. pneumoniae* ATCC BAA-255 RpiB showed the most divergence, with the highest and lowest optimal temperatures of 60 °C and 30 °C, respectively (Feng et al. 2013; Park et al. 2011). Normally, thermostable enzymes are preferred because they cannot only provide the abovementioned advantages in industrial mass production but also exhibit higher evolvability to accept and accumulate more beneficial mutations in protein

Table 1 Comparison of biochemical properties of RpiBs from various microbial sources

Microorganism source	GenBank accession no.	Subunit/total molecular mass (kDa)	Optimum pH	Optimum temperature (°C)	Half-life (h)	K_m (mM)		k_{cat}/K_m (s^{-1} mM^{-1})		Reference
						D-R[b]	D-R5P[c]	D-R[b]	D-R5P[c]	
Clostridium difficile ATCC BAA-1382D-5	CAJ70383.1	17.2/34.4	7.5	40	0.9 (55 °C)	270 ± 1.3	30 ± 1.5	0.6 ± 0.01	500 ± 30	(Yeom et al. 2010)
Clostridium thermocellum ATCC 27405	ABN53797.1	17.0/34.0	7.5	65	96 (50 °C) 18 (55 °C) 8.1 (60 °C) 4.7 (65 °C) 1.7 (70 °C) 0.3 (75 °C)	44 ± 0.7	17 ± 0.4	269 ± 6	3029 ± 107	(Park et al. 2007a; Yoon et al. 2009a)
Ochrobactrum sp. CSL1	ABS15613.1[a]	19.0/72.0	8.0	50	NR	NR	NR	NR	NR	(Shen et al. 2018)
Streptococcus pneumoniae ATCC BAA-255	NP_357883.1	24.0/96.0	7.5	35	15 (40 °C) 6.0 (50 °C)	NR	NR	NR	NR	(Park et al. 2011)
Thermotoga lettingae TMO	ABV32911.1	16.8/35.2	8.0	75	3.3 (75 °C)	NR	NR	NR	NR	(Feng et al. 2013)
Thermotoga maritima ATCC 43589D-5	AAD36157.1	16.7/67.0	8.0	70	3.2 (75 °C)	110 ± 1.0	37 ± 1.8	4.7 ± 0.06	540 ± 32	(Yeom et al. 2010)

[a] The gene encoding the RpiB protein from *Ochrobactrum* sp. CSL1 has the identical sequence with a gene reported in GenBank (accession no. ABS15613.1)

[b] and [c]: D-ribose and D-ribose 5-phosphate

NR not reported

engineering (Bosshart et al. 2015). However, RpiBs from different microorganisms showed significant differences in their thermostability. Specifically, RpiBs from thermophilic and hyperthermophilic bacterium, including *T. lettingae* TMO and *T. maritima* ATCC 43589D-5, exhibited relatively high thermostability, with half-lives of 3.3 and 3.2 h at 75 °C, respectively (Feng et al. 2013; Yeom et al. 2010). In comparison, RpiBs from mesophilic strains showed poor thermostability. For example, the *C. difficile* ATCC BAA-1382D-5 RpiB (Yeom et al. 2010) and the *S. pneumoniae* ATCC BAA-255 RpiB (Park et al. 2011) maintained stable only below 50 °C, with half-lives of 0.9 h at 55 °C and 6.0 h at 50 °C, respectively. According to previous literature, for reducing and inhibiting the Maillard reaction, the temperature for industrial rare sugar production should be controlled appropriately in 60–70 °C (Zhang et al. 2016). Thus, the thermostability of RpiB needs to be improved to satisfy the actual requirements in industrial process.

Generally, metal ions have considerable impacts on monosaccharide isomerases and epimerases such as serving as enzyme activity activator or enhancer, improving thermostability, and reinforcing structural stability (Chen et al. 2018c; Zhang et al. 2013). However, it is intriguing that most of the reported RpiBs were identified as metal-independent enzymes. RpiB from *Ochrobactrum* sp. CSL1 was an exception, which exhibited maximal activity in the presence of Ca^{2+}, but the presence or absence of metal ions had very little impact since it could still maintain 92.50% of native enzyme activity after EDTA treatment (Shen et al. 2018). Because adding metal ions may increase the difficulty in product purification and cause safety problems, RpiBs offer promising advantages over other metal-dependent sugar isomerases for industrial applications.

Substrate specificity, selectivity, and kinetics

Similar to other sugar phosphate isomerases such as mannose-6-phosphate isomerase (Yeom et al. 2009), galactose-6-phosphate isomerase (Park et al. 2007b), and glucose-6-phosphate isomerase (Yoon et al. 2009b), Rpi exhibits very broad substrate specificity. As shown in Table 2, the substrate specificity of different RpiBs varied widely. Although almost all of characterized RpiBs could recognize D-ribose, D-allose, and L-talose as substrates, there existed considerable differences in their specific activities. In addition, the optimal aldose substrate differed according to the microbial origin. For example, RpiBs from *C. difficile* ATCC BAA-1382D-5 (Yeom et al. 2010), *S. pneumoniae* ATCC BAA-255 (Park et al. 2011), and *T. maritima* ATCC 43589D-5 (Yeom et al. 2010) showed the highest specific activity towards D-ribose (53 U mg^{-1}), L-lyxose (27 U mg^{-1}), and L-talose (307 U mg^{-1}), respectively.

Broadly, the substrate selectivity patterns of RpiBs could be divided into two distinct types and, for the sake of convenience, herein named pattern A and pattern B. RpiBs with substrate selectivity of pattern A, like *C. thermocellum* ATCC 27405 RpiB (Park et al. 2007a; Yoon et al. 2009a) and *T. maritima* ATCC 43589D-5 RpiB (Yeom et al. 2010), had the following two characteristics: (1) could only recognize aldoses with hydroxyl groups at C2, C3, and C4 in the same orientation as substrates (Fischer projection); (2) preferred aldose substrates with right-handed configuration at C2, C3, and C4 than those with left-handed configuration (Fig. 1). The substrate selectivity of RpiBs from *C. difficile* ATCC BAA-1382D-5 (Yeom et al. 2010) and *S. pneumoniae* ATCC BAA-255 (Park et al. 2011) were the typical representatives of pattern B (Fig. 1). These enzymes were selective for aldoses with right-handed hydroxyl groups at C2 and C3, including D-ribose, L-talose, D-allose, L-lyxose, L-mannose, and D-gulose. However, the substrate selectivity of the recently reported RpiB from *Ochrobactrum* sp. CSL1 was unconventional. The aldose substrates recognized by all other characterized RpiBs had to fulfill the requirement of possessing identically oriented hydroxyl groups at C2 and C3, while *Ochrobactrum* sp. CSL1 RpiB exhibited activity towards aldoses with different configurations at C2 and C3, like D-arabinose and D-xylose (Shen et al. 2018). Furthermore, *Ochrobactrum* sp. CSL1 RpiB could also isomerize L-rhamnose (a deoxy aldose) into L-rhamnulose, which has not been reported by previously identified RpiBs. Since *C. thermocellum* ATCC 27405 RpiB showed no activity towards L-rhamnose, active sites of these two enzymes were compared. The results showed that two phosphate recognition residues were different in these two enzymes (Arg136 and Asp41 in *C. thermocellum* ATCC 27405 RpiB corresponding to Asn137 and Phe41 in *Ochrobactrum* sp. CSL1 RpiB). The two residues in *Ochrobactrum* sp. CSL1 RpiB were more hydrophobic, which may explain its expanding activity towards L-rhamnose (Park et al. 2007a; Shen et al. 2018). Therefore, like L-rhamnose isomerase from *Caldicellulosiruptor obsidiansis* OB47 (Chen et al. 2018a), the hydrophobic environment may perform a significant impact on the substrate recognition of *Ochrobactrum* sp. CSL1 RpiB.

It is commonly known that Michaelis–Menten constant (K_m) and catalytic efficiency (k_{cat}/K_m) are pivotal parameters for evaluating the catalytic performance of enzymes. As shown in Table 1, the fast enzyme kinetics of *C. thermocellum* ATCC 27405 RpiB were distinctive among all RpiBs (Yoon et al. 2009a). Its k_{cat}/K_m value towards D-ribose was 448 and 57 times higher than that of *C. difficile* ATCC BAA-1382D-5 RpiB and *T. maritima* ATCC 43589D-5 RpiB (Yeom et al. 2010). Further analysis of the three-dimensional structure of *C. thermocellum* ATCC 27405 RpiB revealed that Met94 and Glu97 were responsible for the fast enzyme kinetics. Probably because these two residues can improve the efficiency of sugar-ring opening catalyzing by His98 (Jung et al. 2011). In addition, all of the RpiBs exhibited far lower K_m values and much higher k_{cat}/K_m values to D-ribose 5-phosphate than to D-ribose, indicating that RpiB is one of the enzymes with phosphorylated substrate preference. Obviously, RpiBs with non-phosphorylated substrate preference

Table 2 Specific activities (U mg^{-1}) of different RpiBs for various monosaccharides

Substrate		*C. difficile* ATCC BAA-1382D-5	*C. thermocellum* ATCC 27405	*Ochrobactrum* sp. CSL1	*S. pneumoniae* ATCC BAA-255	*T. maritima* ATCC 43589D-5
Aldose	D-Ribose	53 ± 0.3	5800 ± 64	NR	5.3 ± 0.07	194 ± 2.2
	L-Ribose	ND	272 ± 1.7	6000	ND	4 ± 0.1
	D-Talose	ND	50 ± 0.7	NR	ND	18 ± 0.3
	L-Talose	28 ± 0.5	7363 ± 183	NR	19 ± 0.07	307 ± 5.3
	D-Allose	45 ± 0.1	1352 ± 13	4794	1.9 ± 0.03	23 ± 0.4
	L-Allose	ND	600 ± 12	NR	ND	12 ± 0.1
	D-Lyxose	ND	ND	NR	ND	ND
	L-Lyxose	15 ± 0.1	ND	NR	27 ± 0.05	ND
	D-Mannose	ND	ND	NR	ND	ND
	L-Mannose	NR	ND	NR	2.5 ± 0.05	ND
	D-Gulose	7 ± 0.4	ND	NR	9.6 ± 0.10	ND
	L-Gulose	ND	ND	NR	ND	ND
	D-Xylose	NR	ND	3564	ND	NR
	D-Arabinose	NR	ND	1746	ND	NR
	L-Rhamnose	NR	ND	1770	NR	NR
Ketose	D-Ribulose	120 ± 0.6	5374 ± 110	NR	48 ± 0.08	263 ± 5.4
	L-Ribulose	ND	12 ± 0.07	NR	ND	8 ± 0.1
	D-Tagatose	ND	0.21 ± 0.002	NR	ND	14 ± 0.1
	L-Tagatose	14 ± 0.1	720 ± 21	NR	1.3 ± 0.05	55 ± 0.5
	D-Allulose	3 ± 0.1	1037 ± 15	NR	2.1 ± 0.02	21 ± 0.3
	L-Allulose	ND	0.53 ± 0.009	NR	ND	12 ± 0.1
	D-Xylulose	ND	ND	NR	ND	ND
	L-Xylulose	57 ± 0.4	ND	NR	121 ± 0.10	ND
	D-Fructose	ND	ND	NR	ND	ND
	L-Fructose	9 ± 0.1	ND	NR	1.1 ± 0.02	ND
	D-Sorbose	1 ± 0.1	ND	NR	0.5 ± 0.03	ND
	L-Sorbose	ND	ND	NR	ND	ND
Reference		(Yeom et al. 2010)	(Park et al. 2007a; Yoon et al. 2009a)	(Shen et al. 2018)	(Park et al. 2011)	(Yeom et al. 2010)

One unit (U) is defined as the amount of enzyme required to produce 1 nmol product from substrate per minute

ND: Specific activity was not detected by the analytical method used in the reference

NR not reported

are more suitable for industrial-scale rare sugar production. Therefore, strategy like redesigning the phosphate binding site for obtaining new variants of RpiBs with improved affinity towards non-phosphorylated substrates has been attracting a lot of interest (Yeom et al. 2013).

Crystal structure and molecular modification

Overall structures

There is a large volume of published studies investigating the crystal structures of various Rpis, including eight RpiAs and six RpiBs (Table 3). Interestingly, the overall structures of the same type of Rpi are roughly similar, but RpiA and RpiB show significant structural differences, though they can catalyze the same reaction (Fig. 2). As for RpiA, single subunit, consisting of mixed α-helices and β-strands, contains two domains with different roles. The N-terminal domain with partial key residues is related to catalytic reaction, while the C-terminal domain is responsible for the oligomerization state through the "tetramerization loop," and these two domains are linked via several β-strands (Holmes et al. 2006; Lobley et al. 2012; Strange et al. 2009). Besides, as previously reported, RpiAs from bacteria (*E. coli* K12, *T. thermophilus* HB8, *V. vulnificus* YJ016, and *L. salivarius* UC188) and protozoa (*P. falciparum* 3D7) assembled into dimers, while RpiAs found in archaea (*P. horikoshii* OT3 and *M. jannaschii* MJ1603) and fungi (*S. cerevisiae* S288C) presented in tetramers. The homomultimeric form of RpiAs varied depending

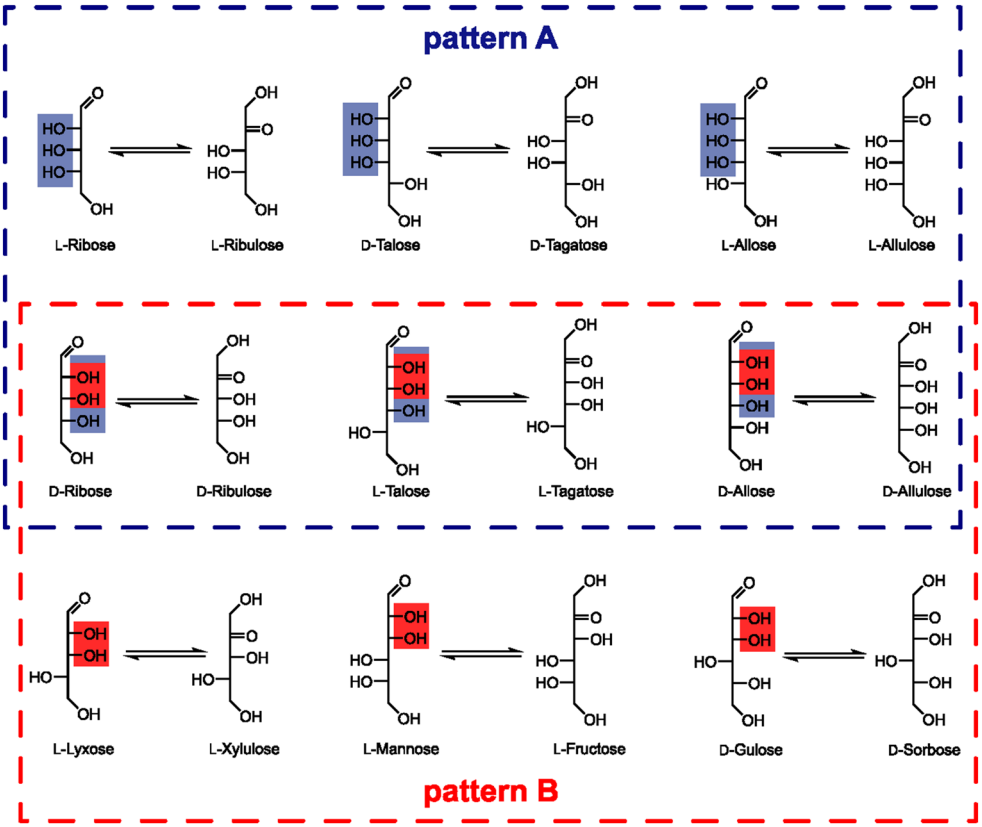

Fig. 1 A schematic diagram for the substrate selectivity patterns of RpiBs. The blue and red boxed structures indicate the specifically recognized hydroxyl group configurations in pattern (A) and pattern (B), respectively

on the length of the "tetramerization loop," and two equal dimers with the longer loop were more likely to generate interaction to form a tetrameric architecture (Graille et al. 2005; Kakuta et al. 2004; Strange et al. 2009).

As for RpiBs, most of them present in the tetrameric forms, except *Mycobacterium tuberculosis* H37Rv RpiB which forms a dimer. And each subunit is folded into a $\alpha\beta\alpha$ sandwich with a five-stranded parallel β-sheet core flanked by three α-helices on each side (Jung et al. 2011; Roos et al. 2005; Stern et al. 2007). In addition, noteworthy is that the active sites of RpiA and RpiB are quite different. First, unlike RpiA forming independent catalytic site in each subunit, the active site of RpiB is located in the border regions of two subunits, composed of residues from both sides. Second, RpiB exhibits a high composition of aromatic residues, whereas RpiA possesses none (Fig. 2). Third, the functions of substrate recognition and catalysis are executed by apparently distinct residues in RpiA and RpiB (Fig. 3).

Catalytic mechanism

Studies on crystal structures of Rpis complexed with substrates, products, or inhibitors have contributed to understand well the catalytic mechanism. Together, these studies indicated that both RpiAs and RpiBs perform the catalytic reaction via two main successive steps: (1) transform the ring form of sugar substrate into the catalytically active linear form; (2) implement aldose-ketose isomerization through 1,2-cis-enediol (ate)–mediated proton transfer. This catalytic mechanism is different from the metal ions required hydride shift mechanism adopted by other isomerases such as L-rhamnose isomerase (Korndorfer et al. 2000) and D-xylose isomerase (Fenn et al. 2004), and to some extent, explained the metal ion independence of Rpis (Soares et al. 2019; Stern et al. 2007). Furthermore, it should be noted that the key residues responsible for ring opening and isomerization in RpiAs and RpiBs are significantly different (Fig. 3). Taking the process of converting R5P to Ru5P as an example, in RpiBs, the furanose ring of R5P opening relies on a histidine (Fig. 3(b)) serving as a general acid for donating a proton to O4 (Roos et al. 2008; Stern et al. 2007). Once the ring is opened, the isomerization step follows immediately which begin with the proton abstraction from C2 performed by the catalytic base (cysteine in all reported RpiBs, except *M. tuberculosis* H37Rv RpiB which using a glutamate as an alternative; Fig. 3(b)). Subsequently, with the participation of a threonine or a serine (Fig. 3(b)), the O1 protonation and O2 deprotonation are in turn carried, accompanied by the forming of enediol (ate) intermediate. Finally, C1 accepts the proton released from the initial catalytic base to form Ru5P (Roos et al. 2008; Wang and Yang 2013; Zhang et al. 2003b). While in

Table 3 Summary of published crystal structures of RpiA and RpiB

	Microorganism source	PDB ID	Resolution (Å)	Mutation or native	Ligand	Reference
RpiA	*Escherichia coli* K12	1LKZ	2.50	Native	–	(Rangarajan et al. 2002)
		1KS2	1.50	Native	–	(Zhang et al. 2003a)
		1O8B	1.25	Native	D-Arabinose-5-phosphate	(Zhang et al. 2003a)
	Lactobacillus salivarius UCC118	4GMK	1.72	Native	Phosphate	(Lobley et al. 2012)
	Methanocaldococcus jannaschii MJ1603	3IXQ	1.78	Native	–	(Strange et al. 2009)
	Plasmodium falciparum 3D7	2F8M	2.09	Native	Phosphate	(Holmes et al. 2006)
	Pyrococcus horikoshii OT3	1LK5	1.75	Native	–	(Ishikawa et al. 2002)
		1LK7	2.00	Native	4-Phospho-D-erythronate	(Ishikawa et al. 2002)
	Saccharomyces cerevisiae S288C	1XTZ	2.10	Native	–	(Graille et al. 2005)
	Thermus thermophilus HB8	1UJ4	1.80	Native	–	(Hamada et al. 2003)
		1UJ5	2.00	Native	D-Ribose-5-phosphate	(Hamada et al. 2003)
		1UJ6	1.74	Native	D-Arabinose-5-phosphate	(Hamada et al. 2003)
	Vibrio vulnificus YJ016	3ENQ	2.00	Native	–	(Kim et al. 2009)
		3ENW	2.00	Native	D-Ribose-5-phosphate	(Kim et al. 2009)
		3ENV	2.00	Native	D-Arabinose-5-phosphate	(Kim et al. 2009)
RpiB	*Clostridium thermocellum* ATCC 27405	3HE8	1.90	Native	–	(Jung et al. 2011)
		3HEE	2.00	Native	D-Ribose-5-phosphate	(Jung et al. 2011)
		3PH3	2.07	Native	D-Ribose	(Jung et al. 2011)
		3PH4	2.07	Native	D-Allose	(Jung et al. 2011)
	Coccidioides immitis RS	3QD5	1.90	Native	–	(Edwards et al. 2011)
		3SDW	1.80	Native	Phosphate	(Edwards et al. 2011)
		3SGW	1.70	Native	Malonic acid	(Edwards et al. 2011)
	Escherichia coli K12	1NN4	2.20	Native	–	(Zhang et al. 2003b)
		2VVR	2.10	Mutant H99N	D-Ribose-5-phosphate	(Roos et al. 2008)
	Mycobacterium tuberculosis H37Rv	1USL	1.88	Native	Phosphate	(Roos et al. 2004)
		2BET	2.20	Native	4-Phospho-D-erythronate	(Roos et al. 2005)
		2BES	2.10	Native	4-Phospho-D-erythronohydroxamic acid	(Roos et al. 2005)
		2VVP	1.65	Native	D-Ribose 5-phosphate D-Ribulose 5-phosphate	(Roos et al. 2008)
		2VVQ	2.00	Native	5-Phospho-D-ribonate	(Roos et al. 2008)
		2VVO	1.85	Native	D-Allose 6-phosphate	(Roos et al. 2008)
	Thermotoga maritima MSB8	1O1X	1.90	Native	–	(Xu et al. 2004)
	Trypanosoma cruzi CL Brener	3K7O	2.00	Native	–	(Stern et al. 2011)
		3K7P	1.40	Mutant C69A	Phosphate	(Stern et al. 2011)
		3K7S	1.90	Native	D-Ribose-5-phosphate	(Stern et al. 2011)
		3K8C	2.10	Native	4-Phospho-D-erythronohydroxamic acid	(Stern et al. 2011)
		3M1P	2.15	Mutant C69A	D-Allose 6-phosphate	(Stern et al. 2011)

"-": Apo structure with no ligand

RpiAs, it has been proposed that the aspartic acid plays a vital role in substrate ring opening and all proton transfers in C1-C2 and O1-O2 are carried by the glutamate (Fig. 3(a)) (Hamada et al. 2003; Zhang et al. 2003a).

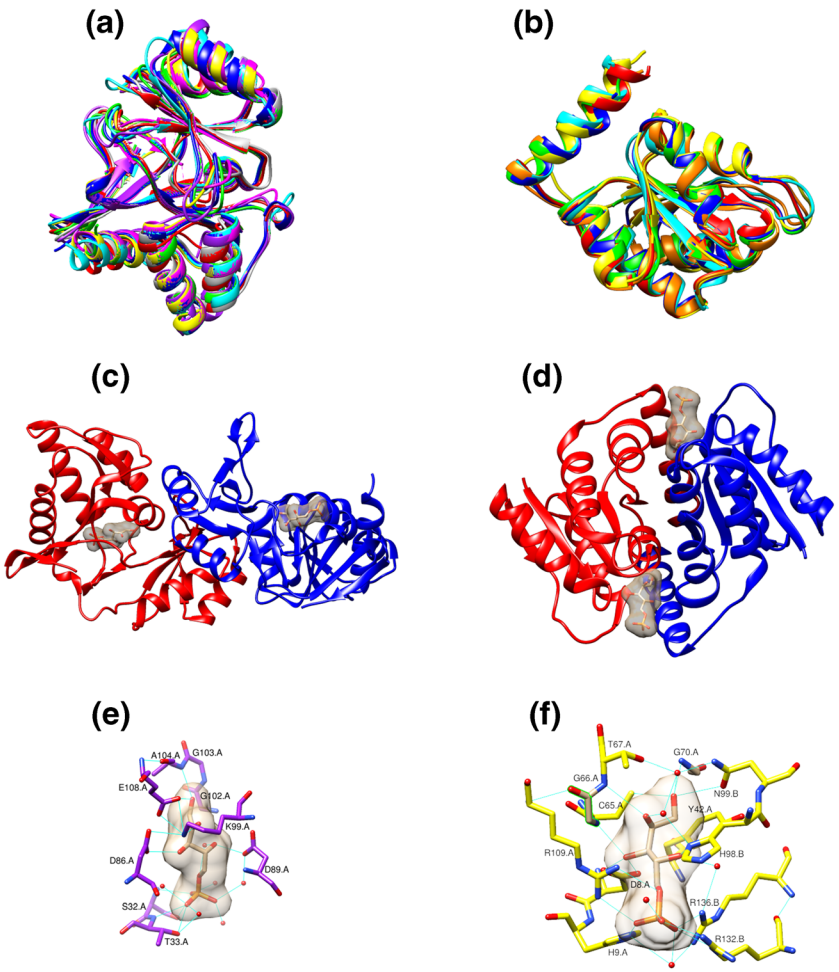

Fig. 2 The three-dimensional structures of RpiAs and RpiBs. (a) and (b) are superimposed diagrams of monomers of RpiAs from *E. coli* (red, 1KS2), *L. salivarius* (yellow, 4GMK), *M. jannaschii* (green, 3IXQ), *P. falciparum* (cyan, 2F8M), *P. horikoshii* (blue, 1LK5), *S. cerevisiae* (purple, 1XTZ), *T. thermophilus* (magenta, 1UJ4), and *V. vulnificus* (gray, 3ENQ) and monomers of RpiBs from *C. thermocellum* (red, 3HE8), *C. immitis* (yellow, 3QD5), *E. coli* (green, 1NN4), *M. tuberculosis* (cyan, 1USL), *T. maritima* (blue, 1O1X), and *T. cruzi* (orange, 3K7O), respectively. (c) and (d) are ribbon representations of the overall structure of R5P-complexed *T. thermophilus* RpiA (1UJ5) and R5P-complexed *C. thermocellum* RpiB (3HEE), respectively. Monomer A is shown in red and monomer B is shown in blue in both structures. (e) and (f) are close-up views of the active sites of *T. thermophilus* RpiA (1UJ5) and *C. thermocellum* RpiB (3HEE) bound to R5P, respectively. All of the stereo views were generated by the program UCSF Chimera

Molecular modification

Consistently, researchers are focusing on molecular modification of enzymes to tailor substrate preferences, ameliorate catalytic properties, and even create new functions. At present, molecular modification of RpiAs has not been explored, but rational design of RpiBs has been reported. In 2011, through structure-based sequence alignment, Stern et al. imitated the phosphate binding loop in *E. coli* RpiB to construct a Δ135E136G mutant of *Trypanosoma cruzi* CL Brener RpiB. Interestingly, this mutant maintained the ability of catalyzing the R5P/Ru5P isomerization and gained the D-allose-6-phosphate isomerase activity which initially did not exist (Stern et al. 2011). Furthermore, using scanning alanine mutagenesis and site-directed mutagenesis, a R132E mutant of *C. thermocellum* ATCC 27405 RpiB and a R133D mutant of *C. difficile* ATCC 43255 RpiB were generated successively by Yeom et al. Due to eliminating the positive charge of the phosphate binding residue Arg, these two mutants showed higher catalytic efficiencies for non-phosphorylated sugars. More specifically, the k_{cat}/K_m values of R132E mutant towards D-allulose and R133D mutant towards D-ribose were 1.5 and 1.8 higher, respectively, compared with those of the corresponding wild-type enzymes (Yeom et al. 2011; Yeom et al. 2013). In addition, Jung et al. transformed two residues of *T. maritima* ATCC 43589D-5 RpiB into corresponding residues of *C. thermocellum* ATCC 27405 RpiB which exhibited the fast enzyme kinetics. As a result, the catalytic activity of L94M mutant and S97E mutant towards D-ribose increased by 75% and 25%, respectively. This result can be explained by the enhancement of ring opening efficiency since these two residues are located nearby the ring opening required residue His (Jung et al. 2011). Therefore, selecting phosphate recognition and ring opening assisted residues as hotspots is considered to be a reasonable strategy for designing improved mutants and can be further used to engineer other Rpis.

Bioproduction of rare sugars by Rpis

Production of D-allose

D-Allose, an aldose with all of the four chiral carbons presenting in the R-configuration, has a bright future for applications

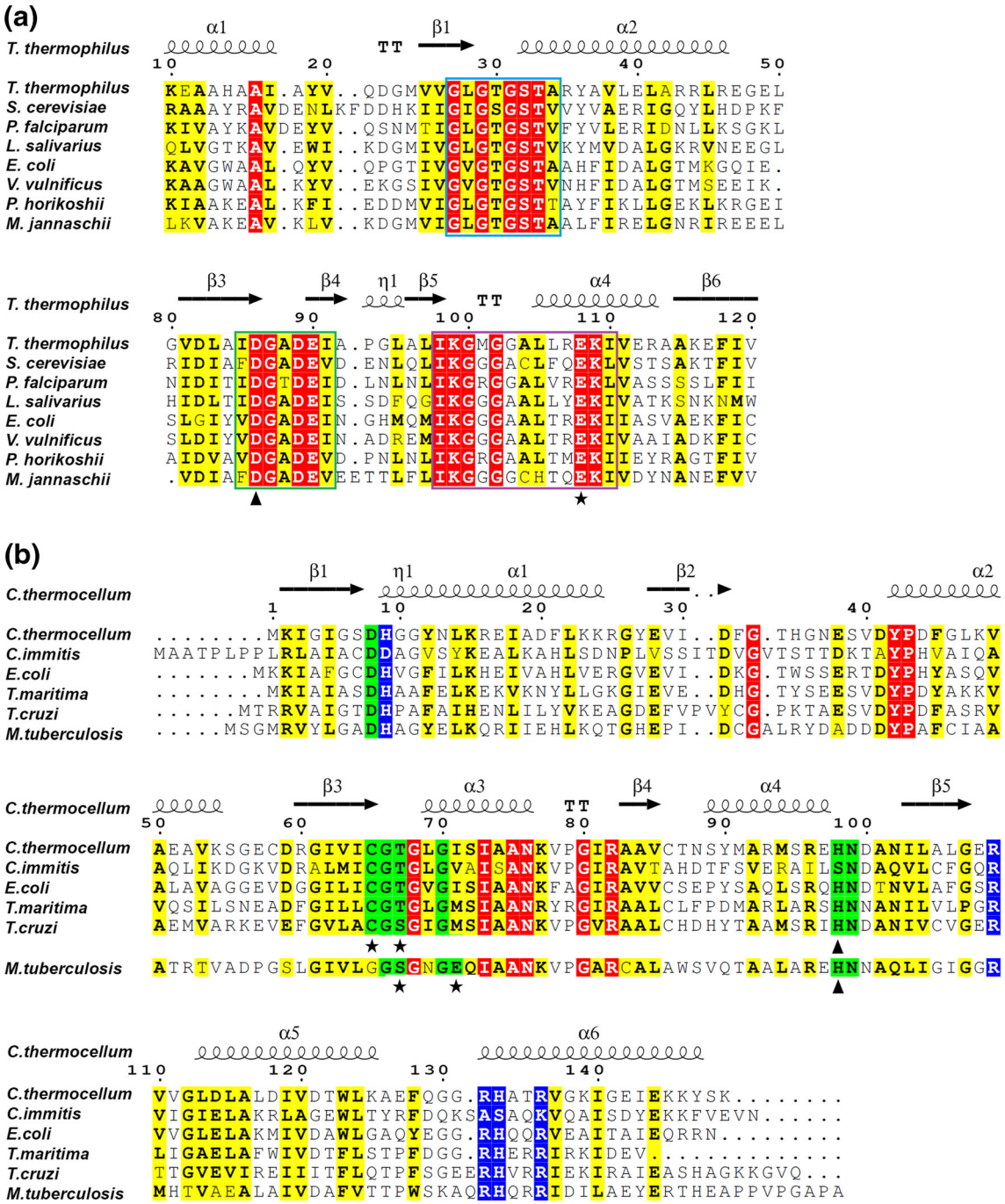

Fig. 3 Structure-based sequence alignments of Table 3–listed RpiAs (a) and RpiBs (b). The blue, green, and purple frames in (a) indicate the phosphate recognition, sugar recognition, and catalysis motifs of RpiAs, respectively. The blue and green boxes in (b) highlight the phosphate binding and sugar binding residues of RpiBs, respectively. The triangle and star in both (a) and (b) mark the ring opening and catalytic residues, respectively. The alignments were prepared using the CLUSTALW and ESPript 3.0 service

in food systems, clinical treatment, and health care due to its unique physicochemical properties and diverse physiological functions. To the best of our knowledge, thus far, biotechnological production of D-allose can only be performed using D-allulose as the substrate. It has been reported that several sugar isomerases possess the catalytic ability for isomerizing D-allulose into D-allose such as L-rhamnose isomerase (Xu et al. 2017), D-galactose-6-phosphate isomerase (Park et al. 2007b), and RpiB. The first application of RpiB for D-allose production was carried out by Park et al. in 2007. Under the optimized conditions of pH 7.5, 50 °C, and 500 g L^{-1} D-allulose, RpiB from *C. thermocellum* ATCC 27405 produced 165 g L^{-1} D-allose in 6 h, with an overall yield of 33% (Park et al. 2007a). Four years later, through rational design, a single-

site mutant (R132E) of *C. thermocellum* ATCC 27405 RpiB was obtained which exhibited a 7% increase in conversion yield comparing with the wild-type enzyme under the same reaction conditions and enzyme concentration (Yeom et al. 2011). In addition, by using purified RpiB from *T. lettingae* TMO, the sole product D-allose could be formed in the presence of 100 mM D-allulose at pH 8.0 and 55 °C, and the final reaction equilibrium approached at 4 h, with a ratio of 32:68 between D-allose and D-allulose. Furthermore, by whole-cell transformation using recombinant *E. coli* cells expressing RpiB from *T. lettingae* TMO, after 24 h, 28 g L^{-1} D-allose could be obtained from 100 g L^{-1} D-allulose in a 1-L reaction system, at pH 8.0 and 55 °C (Feng et al. 2013). Since D-allulose is very scarce and expensive, directly using D-allulose as a substrate for industrial-scale D-allose production would be unrealistic. To decrease the production cost, recently, Lee et al. established a two-enzyme system for D-allose production from D-fructose by coupling the enzymatic epimerization catalyzed by D-allulose 3-epimerase (DAE) and isomerization catalyzed by RpiB. Under the optimized conditions of pH 7.5, 60 °C, 1 mM Co^{2+}, and 600 g L^{-1} D-fructose, 0.1 g L^{-1} DAE from *Flavonifractor plautii* ATCC 29863 and 12 g L^{-1} RpiB from *C. thermocellum* ATCC 27405 were added sequentially or simultaneously, with an overall conversion yield of 32% and 42%, respectively (Lee et al. 2018). In addition, integration of the two-enzyme cascade reaction and product separation into a continuous process by using simulated moving bed chromatography may further improve the conversion yield (Morimoto et al. 2006; Wagner et al. 2015).

Production of L-sugars

As mentioned above, L-series sugars have emerged as important starting materials for the synthesis of diverse compounds with special functions and commercial value. Recently, due to the broad substrate specificity, RpiB has also been utilized for several L-form rare sugars, including L-rhamnulose, L-lyxose, and L-tagatose. L-Rhamnulose (6-deoxy-L-fructose) could be produced from L-rhamnose by *Ochrobactrum* sp. CSL1 RpiB and the highest production was observed at pH 8.0, 50 °C, and 1 mM Ca^{2+} for 4.5 h, with a conversion yield of 26% (Shen et al. 2018). RpiB from *S. pneumoniae* ATCC BAA-255 could produce 350 g L^{-1} L-lyxose from 500 g L^{-1} L-xylulose in 3 h at pH 7.5 and 35 °C, with a volumetric productivity of 117 g L^{-1} h^{-1} and a conversion yield of 70% (Park et al. 2011). As for enzymatic production of L-tagatose, *C. thermocellum* ATCC 27405 RpiB catalyzed the isomerization of L-talose to L-tagatose, with a conversion yield of 89%, at pH 7.5 and 50 °C in about 1.5 h (Yoon et al. 2009a). And 450 g L^{-1} L-tagatose could be obtained from 500 g L^{-1} L-talose by 600 U mL^{-1} *S. pneumoniae* ATCC BAA-255 RpiB at pH 7.5 and 35 °C after 5 h, and a 90% conversion yield with a volumetric productivity of 90 g L^{-1} h^{-1} was achieved (Park et al. 2011). It is worth mentioning that there were no byproducts formed in all of the aforementioned production processes, indicating that RpiB is an ideal L-sugar producer.

Rpi as a potential drug target against trypanosomatids

Due to the unsatisfactory efficacy and severe side effects of current chemotherapeutic agents for treatment of trypanosomatid-caused diseases, searching rational molecular targets and designing target specifically inhibitory drugs are imperative. Considering the critical role of Rpi in the pentose phosphate pathway, researchers have explored the impact of Rpi on different trypanosomatids. Through RNAi-based gene silencing, Loureiro et al. (2015) demonstrated that *Trypanosoma brucei* Rpi significantly affected the in vitro growth and in vivo infectivity of *T. brucei* (a trypanosomatid of the *Trypanosoma* genus). Moreover, the study by Faria et al. (2016) suggested that Rpi was necessary for the survival of *Leishmania infantum* (a trypanosomatid of the *Leishmania* genus) since Rpi inactivated mutants could not be constructed unless an episomal copy of Rpi gene was provided. The essentiality of Rpi for trypanosomatids favors it as a potential drug target candidate. However, it should be noted that previous studies have shown that human Rpi was related to hepatocarcinogenesis (Ciou et al. 2015) and human deficient in Rpi would present progressive leukoencephalopathy and peripheral neuropathy (Huck et al. 2004; Kaur et al. 2019). Consequently, new drugs aiming at Rpi need to be highly selective and be able to specifically inhibit the Rpi of trypanosomatids, with little/no influence on human Rpi in the meanwhile. Fortunately, designing such specific inhibitors is theoretically feasible since the Rpis of trypanosomatids and human host belong to type B and type A, respectively, and their active sites are sufficiently different (Capriles et al. 2015; Sinatti et al. 2017). Up to now, several compounds have shown inhibitory activity against trypanosomatid RpiB, including 4-phospho-D-erythronate, 4-phospho-D-erythronohydroxamic acid, and D-allose-6-phosphate (Stern et al. 2007; Stern et al. 2011). More recently, two novel compounds (ZINC ID 36975961 and 43763931) were identified as promising inhibitors of trypanosomatid RpiB by Sinatti et al. (2017) via pharmacophore modeling, molecular docking, and molecular dynamic simulations. Although there is still a sizable gap between the inhibitory effects and the requirement for clinical application, these compounds provide good references for future work in drug design.

Authors' contributions JC wrote the manuscript and drew the figures. HW contributed to manuscript editing. WZ and WM designed, supervised, and revised the manuscript. All authors read and approved the manuscript.

Funding information This study was funded by the National Natural Science Foundation of China (Nos. 31801583 and 31922073), the Natural Science Foundation of Jiangsu Province (No. BK20180607), and the National First-Class Discipline Program of Food Science and Technology of China (JUFSTR20180203).

Compliance with ethical standards

Conflict of interest The authors declare that they have no conflict of interest.

Ethical approval This article does not contain any studies with human participants or animals performed by any of the authors.

References

Bosshart A, Hee CS, Bechtold M, Schirmer T, Panke S (2015) Directed divergent evolution of a thermostable D-tagatose epimerase towards improved activity for two hexose substrates. ChemBioChem 16(4): 592–601. https://doi.org/10.1002/cbic.201402620

Capriles P, Baprista LPR, Guedes IA, Guimaraes ACR, Custodio FL, Alves-Ferreira M, Dardenne LE (2015) Structural modeling and docking studies of ribose 5-phosphate isomerase from *Leishmania major* and *Homo sapiens*: a comparative analysis for Leishmaniasis treatment. J Mol Graph 55:134–147. https://doi.org/10.1016/j.jmgm.2014.11.002

Chen ZW, Chen JJ, Zhang WL, Zhang T, Guang C, Mu WM (2018a) Improving thermostability and catalytic behavior of L-rhamnose isomerase from *Caldicellulosiruptor obsidiansis* OB47 toward D-allulose by site-directed mutagenesis. J Agric Food Chem 66(45): 12017–12024. https://doi.org/10.1021/acs.jafc.8b05107

Chen ZW, Chen JJ, Zhang WL, Zhang T, Guang C, Mu WM (2018b) Recent research on the physiological functions, applications, and biotechnological production of D-allose. Appl Microbiol Biotechnol 102(10):4269–4278. https://doi.org/10.1007/s00253-018-8916-6

Chen ZW, Xu W, Zhang WL, Zhang T, Jiang B, Mu WM (2018c) Characterization of a thermostable recombinant L-rhamnose isomerase from *Caldicellulosiruptor obsidiansis* OB47 and its application for the production of L-fructose and L-rhamnulose. J Sci Food Agric 98(6):2184–2193. https://doi.org/10.1002/jsfa.8703

Ciou SC, Chou YT, Liu YL, Nieh YC, Lu JW, Huang SF, Chou YT, Cheng LH, Lo JF, Chen MJ, Yang MC, Yuh CH, Wang HD (2015) Ribose-5-phosphate isomerase a regulates hepatocarcinogenesis via PP2A and ERK signaling. Int J Cancer 137(1):104–115. https://doi.org/10.1002/ijc.29361

Edwards TE, Abramov AB, Smith ER, Baydo RO, Leonard JT, Leibly DJ, Thompkins KB, Clifton MC, Gardberg AS, Staker BL, Van Voorhis WC, Myler PJ, Stewart LJ (2011) Structural characterization of a ribose-5-phosphate isomerase B from the pathogenic fungus *Coccidioides immitis*. BMC Struct Biol 11(1):39–47. https://doi.org/10.1186/1472-6807-11-39

Fan C, Xu W, Zhang T, Zhou L, Jiang B, Mu WM (2015) Engineering of *Alicyclobacillus hesperidum* L-arabinose isomerase for improved catalytic activity and reduced pH optimum using random and site-directed mutagenesis. Appl Biochem Biotechnol 177(7):1480–1492. https://doi.org/10.1007/s12010-015-1828-3

Faria J, Loureiro I, Santarem N, Cecilio P, Macedo-Ribeiro S, Tavares J, Cordeiro-Da-Silva A (2016) Disclosing the essentiality of ribose-5-phosphate isomerase B in trypanosomatids. Sci Rep 6:26937–23952. https://doi.org/10.1038/srep26937

Feng Z, Mu W, Jiang B (2013) Characterization of ribose-5-phosphate isomerase converting D-psicose to D-allose from *Thermotoga lettingae* TMO. Biotechnol Lett 35(5):719–724. https://doi.org/10.1007/s10529-013-1136-3

Fenn TD, Ringe D, Petsko GA (2004) Xylose isomerase in substrate and inhibitor Michaelis states: atomic resolution studies of a metal-mediated hydride shift. Biochemistry 43(21):6464–6474. https://doi.org/10.1021/bi049812o

Graille M, Meyer P, Leulliot N, Sorel I, Janin J, Van Tilbeurgh H, Quevillon-Cheruel S (2005) Crystal structure of the *S. cerevisiae* D-ribose-5-phosphate isomerase: comparison with the archaeal and bacterial enzymes. Biochimie 87(8):763–769. https://doi.org/10.1016/j.biochi.2005.03.001

Granstrom TB, Takata G, Tokuda M, Izumori K (2004) Izumoring: a novel and complete strategy for bioproduction of rare sugars. J Biosci Bioeng 97(2):89–94. https://doi.org/10.1016/s1389-1723(04)70173-5

Hamada K, Ago H, Sugahara M, Nodake Y, Kuramitsu S, Miyano M (2003) Oxyanion hole-stabilized stereospecific isomerization in ribose-5-phosphate isomerase (Rpi). J Biol Chem 278(49):49183–49190. https://doi.org/10.1074/jbc.M309272200

Hecquet L, Bolte J, Demuynck C (1996) Enzymatic synthesis of "natural-labeled" 6-deoxy-L-sorbose precursor of an important food flavor. Tetrahedron 52(24):8223–8232. https://doi.org/10.1016/0040-4020(96)00379-1

Hofmann C, Boll R, Heitmann B, Hauser G, Durr C, Frerich A, Weitnauer G, Glaser SJ, Bechthold A (2005) Genes encoding enzymes responsible for biosynthesis of L-lyxose and attachment of eurekanate during avilamycin biosynthesis. Chem Biol 12(10): 1137–1143. https://doi.org/10.1016/j.chembiol.2005.08.016

Holmes MA, Buckner FS, Van Voorhis WC, Verlinde C, Mehlin C, Boni E, DeTitta G, Luft J, Lauricella A, Anderson L, Kalyuzhniy O, Zucker F, Schoenfeld LW, Earnest TN, Hol WGJ, Merritt EA (2006) Structure of ribose 5-phosphate isomerase from *Plasmodium falciparum*. Acta Crystallogr F-Struct Biol Commun 62(5):427–431. https://doi.org/10.1107/s1744309106010876

Huck JHJ, Verhoeven NM, Struys EA, Salomons GS, Jakobs C, van der Knaap MS (2004) Ribose-5-phosphate isomerase deficiency: new inborn error in the pentose phosphate pathway associated with a slowly progressive leukoencephalopathy. Am J Hum Genet 74(4): 745–751. https://doi.org/10.1086/383204

Ishikawa K, Matsui I, Payan F, Cambillau C, Ishida H, Kawarabayasi Y, Kikuchi H, Roussel A (2002) A hyperthermostable D-ribose-5-phosphate isomerase from *Pyrococcus horikoshii* characterization and three-dimensional structure. Structure 10(6):877–886. https://doi.org/10.1016/s0969-2126(02)00779-7

Izumori K (2002) Bioproduction strategies for rare hexose sugars. Naturwissenschaften 89(3):120–124. https://doi.org/10.1007/s00114-002-0297-z

Jenkinson SF, Fleet GWJ, Nash RJ, Koike Y, Adachi I, Yoshihara A, Morimoto K, Izumori K, Kato A (2011) Looking-glass synergistic pharmacological chaperones: DGJ and L-DGJ from the enantiomers of tagatose. Org Lett 13(15):4064–4067. https://doi.org/10.1021/ol201552q

Jung CH, Hartman FC, Lu TYS, Larimer FW (2000) D-ribose-5-phosphate isomerase from spinach: heterologous overexpression, purification, characterization, and site-directed mutagenesis of the recombinant enzyme. Arch Biochem Biophys 373(2):409–417. https://doi.org/10.1006/abbi.1999.1554

Jung J, Kim JK, Yeom SJ, Ahn YJ, Oh DK, Kang LW (2011) Crystal structure of *Clostridium thermocellum* ribose-5-phosphate isomerase B reveals properties critical for fast enzyme kinetics. Appl Microbiol Biotechnol 90(2):517–527. https://doi.org/10.1007/s00253-011-3095-8

Kakuta Y, Tahara M, Maetani S, Yao M, Tanaka I, Kimura M (2004) Crystal structure of the regulatory subunit of archaeal initiation factor 2B (aIF2B) from hyperthermophilic archaeon *Pyrococcus horikoshii* OT3: a proposed structure of the regulatory subcomplex

of eukaryotic IF2B. Biochem Biophys Res Commun 319(3):725–732. https://doi.org/10.1016/j.bbrc.2004.05.045

Kaur P, Wamelink MMC, van der Knaap MS, Girisha KM, Shukla A (2019) Confirmation of a rare genetic leukoencephalopathy due to a novel biallelic variant in RPIA. Eur J Med Genet 62(8):103708–103711. https://doi.org/10.1016/j.ejmg.2019.103708

Kim TG, Kwon TH, Min K, Dong MS, Park YI, Ban C (2009) Crystal structures of substrate and inhibitor complexes of ribose 5-phosphate isomerase a from *Vibrio vulnificus* YJ016. Mol Cells 27(1):99–103. https://doi.org/10.1007/s10059-009-0010-6

Korndorfer IP, Fessner WD, Matthews BW (2000) The structure of rhamnose isomerase from *Escherichia coli* and its relation with xylose isomerase illustrates a change between inter and intra-subunit complementation during evolution. J Mol Biol 300(4):917–933. https://doi.org/10.1006/jmbi.2000.3896

Kovarova J, Barrett MP (2016) The pentose phosphate pathway in parasitic trypanosomatids. Trends Parasitol 32(8):622–634. https://doi.org/10.1016/j.pt.2016.04.010

Kwon SY, Baek HH (2014) Effects of temperature, pH, organic acids, and sulfites on tagatose browning in solutions during processing and storage. Food Sci Biotechnol 23(3):677–684. https://doi.org/10.1007/s10068-014-0092-6

Lee TE, Shin KC, Oh DK (2018) Biotransformation of fructose to allose by a one-pot reaction using *Flavonifractor plautii* D-allulose 3-epimerase and *Clostridium thermocellum* ribose 5-phosphate isomerase. J Microbiol Biotechnol 28(3):418–424. https://doi.org/10.4014/jmb.1709.09044

Lobley CMC, Aller P, Douangamath A, Reddivari Y, Bumann M, Bird LE, Nettleship JE, Brandao-Neto J, Owens RJ, O'Toole PW, Walsh MA (2012) Structure of ribose 5-phosphate isomerase from the probiotic bacterium *Lactobacillus salivarius* UCC118. Acta Crystallogr F-Struct Biol Commun 68(12):1427–1433. https://doi.org/10.1107/s174430911204273x

Loureiro I, Faria J, Clayton C, Macedo-Ribeiro S, Santarem N, Roy N, Cordeiro-Da-Siva A, Tavares J (2015) Ribose 5-phosphate isomerase B knockdown compromises *Trypanosoma brucei* bloodstream form infectivity. Plos Neglect Trop Dis 9(1):e3430–e3440. https://doi.org/10.1371/journal.pntd.0003430

Morimoto K, Park CS, Ozaki M, Takeshita K, Shimonishi T, Granstrom TB, Takata G, Tokuda M, Izumori K (2006) Large scale production of D-allose from D-psicose using continuous bioreactor and separation system. Enzym Microb Technol 38(6):855–859. https://doi.org/10.1016/j.enzmictec.2005.08.014

Park CS, Yeom SJ, Kim HJ, Lee SH, Lee JK, Kim SW, Oh DK (2007a) Characterization of ribose-5-phosphate isomerase of *Clostridium thermocellum* producing D-allose from D-psicose. Biotechnol Lett 29(9):1387–1391. https://doi.org/10.1007/s10529-007-9393-7

Park HY, Park CS, Kim HJ, Oh DK (2007b) Substrate specificity of a galactose 6-phosphate isomerase from *Lactococcus lactis* that produces D-allose from D-psicose. J Biotechnol 132(1):88–95. https://doi.org/10.1016/j.jbiotec.2007.08.022

Park CS, Yeom SJ, Lim YR, Kim YS, Oh DK (2011) Substrate specificity of a recombinant ribose-5-phosphate isomerase from *Streptococcus pneumoniae* and its application in the production of L-lyxose and L-tagatose. World J Microbiol Biotechnol 27(4):743–750. https://doi.org/10.1007/s11274-010-0511-7

Poulsen TS, Chang YY, Hove-Jensen B (1999) D-Allose catabolism of *Escherichia coli*: involvement of alsI and regulation of als regulon expression by allose and ribose. J Bacteriol 181(22):7126–7130. https://doi.org/10.1128/jb.181.22.7126-7130.1999

Rangarajan ES, Sivaraman J, Matte A, Cygler M (2002) Crystal structure of D-ribose-5-phosphate isomerase (RpiA) from *Escherichia coli*. Proteins 48(4):737–740. https://doi.org/10.1002/prot.10203

Roos AK, Andersson CE, Bergfors T, Jacobsson M, Karlen A, Unge T, Jones TA, Mowbray SL (2004) *Mycobacterium tuberculosis* ribose-5-phosphate isomerase has a known fold, but a novel active site. J Mol Biol 335(3):799–809. https://doi.org/10.1016/j.jmb.2003.11.021

Roos AK, Burgos E, Ericsson DJ, Salmon L, Mowbray SL (2005) Competitive inhibitors of *Mycobacterium tuberculosis* ribose-5-phosphate isomerase B reveal new information about the reaction mechanism. J Biol Chem 280(8):6416–6422. https://doi.org/10.1074/jbc.M412018200

Roos AK, Mariano S, Kowalinski E, Salmon L, Mowbray SL (2008) D-Ribose-5-phosphate isomerase B from *Escherichia coli* is also a functional D-allose-6-phosphate isomerase, while the *Mycobacterium tuberculosis* enzyme is not. J Mol Biol 382(3):667–679. https://doi.org/10.1016/j.jmb.2008.06.090

Shen M, Ju X, Xu XQ, Yao X, Li L, Chen J, Hu C, Fu J, Yan L (2018) Characterization of ribose-5-phosphate isomerase B from newly isolated strain *Ochrobactrum* sp CSL1 producing L-rhamnulose from L-rhamnose. J Microbiol Biotechnol 28(7):1122–1132. https://doi.org/10.4014/jmb.1802.02021

Sinatti VDC, Baptista LPR, Alves-Ferreira M, Dardenne L, da Silva JHM, Guimaraes AC (2017) In silico identification of inhibitors of ribose 5-phosphate isomerase from *Trypanosoma cruzi* using ligand and structure based approaches. J Mol Graph 77:168–180. https://doi.org/10.1016/j.jmgm.2017.08.007

Soares RF, Antunes D, Santos LHS, Rocha GV, Bastos LS, Guimaraes ACR, Caffarena ER (2019) Studying effects of different protonation states of His11 and His102 in ribose-5-phosphate isomerase of *Trypanosoma cruzi*: an example of cooperative behavior. J Biomol Struct Dyn 38:1–10. https://doi.org/10.1080/07391102.2019.1626769

Stern AL, Burgos E, Salmon L, Cazzulo JJ (2007) Ribose 5-phosphate isomerase type B from *Trypanosoma cruzi*: kinetic properties and site-directed mutagenesis reveal information about the reaction mechanism. Biochem J 401(1):279–285. https://doi.org/10.1042/bj20061049

Stern AL, Naworyta A, Cazzulo JJ, Mowbray SL (2011) Structures of type B ribose 5-phosphate isomerase from *Trypanosoma cruzi* shed light on the determinants of sugar specificity in the structural family. FEBS J 278(5):793–808. https://doi.org/10.1111/j.1742-4658.2010.07999.x

Stincone A, Prigione A, Cramer T, Wamelink MMC, Campbell K, Cheung E, Olin-Sandoval V, Gruning NM, Kruger A, Alam MT, Keller MA, Breitenbach M, Brindle KM, Rabinowitz JD, Ralser M (2015) The return of metabolism: biochemistry and physiology of the pentose phosphate pathway. Biol Rev 90(3):927–963. https://doi.org/10.1111/brv.12140

Strange RW, Antonyuk SV, Ellis MJ, Bessho Y, Kuramitsu S, Yokoyama S, Hasnain SS (2009) The structure of an archaeal ribose-5-phosphate isomerase from *Methanocaldococcus jannaschii* (MJ1603). Acta Crystallogr F-Struct Biol Commun 65(12):1214–1217. https://doi.org/10.1107/s1744309109044923

Wagner N, Bosshart A, Failmezger J, Bechtold M, Panke S (2015) A separation-integrated cascade reaction to overcome thermodynamic limitations in rare-sugar synthesis. Angew Chem-Int Edit 54(14):4182–4186. https://doi.org/10.1002/anie.201411279

Wang J, Yang W (2013) Concerted proton transfer mechanism of *Clostridium thermocellum* ribose-5-phosphate isomerase. J Phys Chem B 117(32):9354–9361. https://doi.org/10.1021/jp404948c

Xu Q, Schwarzenbacher R, McMullan D, von Delft F, Brinen LS, Canaves JM, Dai XP, Deacon AM, Elsliger MA, Eshagi S, Floyd R, Godzik A, Grittini C, Grzechnik SK, Jaroszewski L, Karlak C, Klock HE, Koesema E, Kovarik JS, Kreusch A, Kuhn P, Lesley SA, Levin I, TM MP, Miller MD, Morse A, Moy K, Ouyang J, Page R, Quijano K, Robb A, Spraggon G, Stevens RC, van den Bedem H, Velasquez J, Vincent J, Wang XH, West B, Wolf G, Hodgson KO, Wooley J, Wilson IA (2004) Crystal structure of a ribose-5-phosphate isomerase RpiB (TM1080) from *Thermotoga maritima*

at 1.90 angstrom resolution. Proteins 56(1):171–175. https://doi.org/10.1002/prot.20129

Xu W, Zhang W, Zhang T, Jiang B, Mu W (2016) L-Rhamnose isomerase and its use for biotechnological production of rare sugars. Appl Microbiol Biotechnol 100(7):2985–2992. https://doi.org/10.1007/s00253-016-7369-z

Xu W, Zhang W, Tian Y, Zhang T, Jiang B, Mu W (2017) Characterization of a novel thermostable L-rhamnose isomerase from *Thermobacillus composti* KWC4 and its application for production of D-allose. Process Biochem 53:153–161. https://doi.org/10.1016/j.procbio.2016.11.025

Yeom SJ, Kim NH, Yoon RY, Kwon HJ, Park CS, Oh DK (2009) Characterization of a mannose-6-phosphate isomerase from *Geobacillus thermodenitrificans* that converts monosaccharides. Biotechnol Lett 31(8):1273–1278. https://doi.org/10.1007/s10529-009-0003-8

Yeom SJ, Kim BN, Park CS, Oh DK (2010) Substrate specificity of ribose-5-phosphate isomerases from *Clostridium difficile* and *Thermotoga maritima*. Biotechnol Lett 32(6):829–835. https://doi.org/10.1007/s10529-010-0224-x

Yeom SJ, Seo ES, Kim YS, Oh DK (2011) Increased D-allose production by the R132E mutant of ribose-5-phosphate isomerase from *Clostridium thermocellum*. Appl Microbiol Biotechnol 89(6):1859–1866. https://doi.org/10.1007/s00253-010-3026-0

Yeom SJ, Kim YS, Oh DK (2013) Development of novel sugar isomerases by optimization of active sites in phosphosugar isomerases for monosaccharides. Appl Environ Microbiol 79(3):982–988. https://doi.org/10.1128/aem.02539-12

Yoon RY, Yeom SJ, Kim HJ, Oh DK (2009a) Novel substrates of a ribose-5-phosphate isomerase from *Clostridium thermocellum*. J Biotechnol 139(1):26–32. https://doi.org/10.1016/j.jbiotec.2008.09.012

Yoon RY, Yeom SJ, Park CS, Oh DK (2009b) Substrate specificity of a glucose-6-phosphate isomerase from *Pyrococcus furiosus* for monosaccharides. Appl Microbiol Biotechnol 83(2):295–303. https://doi.org/10.1007/s00253-009-1859-1

Zhang RG, Andersson CE, Savchenko A, Skarina T, Evdokimova E, Beasley S, Arrowsmith CH, Edwards AM, Joachimiak A, Mowbray SL (2003a) Structure of *Escherichia coli* ribose-5-phosphate isomerase: a ubiquitous enzyme of the pentose phosphate pathway and the Calvin cycle. Structure 11(1):31–42. https://doi.org/10.1016/s0969-2126(02)00933-4

Zhang RG, Andersson CE, Skarina T, Evdokimova E, Edwards AM, Joachimiak A, Savchenko A, Mowbray SL (2003b) The 2.2 angstrom resolution structure of RpiB/AlsB from *Escherichia coli* illustrates a new approach to the ribose-5-phosphate isomerase reaction. J Mol Biol 332(5):1083–1094. https://doi.org/10.1016/j.jmb.2003.08.009

Zhang W, Fang D, Xing Q, Zhou L, Jiang B, Mu W (2013) Characterization of a novel metal-dependent D-psicose 3-epimerase from *Clostridium scindens* 35704. PLoS One 8(4):e62987–e62995. https://doi.org/10.1371/journal.pone.0062987

Zhang W, Yu S, Zhang T, Jiang B, Mu W (2016) Recent advances in D-allulose: physiological functionalities, applications, and biological production. Trends Food Sci Technol 54:127–137. https://doi.org/10.1016/j.tifs.2016.06.004

Zhang W, Zhang T, Jiang B, Mu W (2017) Enzymatic approaches to rare sugar production. Biotechnol Adv 35(2):267–274. https://doi.org/10.1016/j.biotechadv.2017.01.004